Fluidized-Bed MOCVD of Bi2O3 Thin Films from Bismuth Triphenyl under Atmospheric Pressure

Nicolas Reuge, Jeannette Dexpert-Ghys, Brigitte Caussat

Fluidized-Bed MOCVD of Bi_2O_3 Thin Films from Bismuth Triphenyl under Atmospheric Pressure**

By *Nicolas Reuge*, *Jeannette Dexpert-Ghys*, and *Brigitte Caussat**

Bismuth oxide thin films are of great interest due to their significant band gap, high refractive index, and dielectric permittivity, as well as marked photoconductivity and photoluminescence.[1] These properties make Bi_2O_3 films well suited for many applications such as microelectronics,[2] sensor technology,[3] optical coatings,[4] and ceramic glass manufacturing.[5]

Various precursors have been employed to synthesize Bi_2O_3 films by CVD, including bismuth halides and bismuth triphenyl $Bi(Ph)_3$.[1,2,4,6–11] Halides are known to be toxic and corrosive. $Bi(Ph)_3$ is safer and offers remarkable advantages in terms of thermal stability and clean sublimation.[1] $Bi(Ph)_3$ is solid at ambient temperature and liquefies from 80 °C. In its gaseous state, when diluted in a neutral gas such as nitrogen and in the presence of oxygen, it reacts heterogeneously with this latter, at temperatures higher than 350 °C, to form solid Bi_2O_3.[1]

Earlier reports[12] have identified four possible crystalline phases in micro-crystalline samples. The ''α'' monoclinic form is stable at room temperature; it transforms into δ (cubic) at 729 °C. Two intermediate metastable phases, β (tetragonal) or γ (cubic), may appear when cooling down; each returning to the α phase at room temperature. However, each of the crystalline phases α, β, γ, δ, or a mixture of some or all of them, have been observed at room temperature when more or less thin films have been investigated.[1,2,11] More recently, ω (triclinic, metastable) and ε (orthorhombic) have also been referenced.[9] Therefore, the type of the deposited crystalline phase depends strongly on the experimental conditions and on the nature of the substrate.

[*] Dr B. Caussat, Dr N. Reuge
Laboratoire de Génie Chimique, UMR CNRS 5503, Université de Toulouse, INPT, ENSIACET
4, Allée Emile Monso, BP 84234, 31432 Toulouse Cedex 4 (France)
E-mail: Brigitte.Caussat@ensiacet.fr
Dr J. Dexpert-Ghys
CEMES, UPR CNRS 8011
29 rue Jeanne Marvig, 31055 Toulouse Cedex (France)

[**] This project has been supported by the French Agence Nationale de la Recherche, Réseau National Matériaux et Procédés (ANR RNMP05-PRONANOX), and by the Midi-Pyrénées Regional Council.

To our knowledge, only three teams have studied Bi_2O_3 CVD from $Bi(Ph)_3$; in all cases on planar substrates and under reduced pressure. Bandoli et al.[2] and Barreca et al.[10] performed MOCVD of Bi_2O_3 on SiO_2 and Al_2O_3 substrates, under low pressure (6–12 mbar) and at 420 °C, with several oxygen flow rates. Bandoli et al. showed that the crystalline phase (α or β Bi_2O_3) depends on the O_2 flow rate and on the nature of the substrate. On Al_2O_3 substrates, the α phase is predominant at low oxygen inlet concentration, whereas the β phase appears with higher oxygen flow rates. Bedoya et al.[1] worked between 350 and 550 °C under the same range of pressure on Pt and Ir substrates. They showed that without O_2, no precursor decomposition occurs. An unambiguous determination of the crystalline phases was difficult due to the poor quality of crystallization. α-Bi_2O_3 was always observed at the higher deposition temperature, whereas at lower deposition temperatures, mixtures of β and γ were identified. The crystallites were smaller on Ir (10 nm) than on Pt (25–35 nm) for temperatures below 450 °C, and they were of similar size on the two substrates (40 nm) beyond 450 °C.

In this work, we report the synthesis of Bi_2O_3 films on alumina particles using fluidized bed (FB) CVD under atmospheric pressure. Bismuth triphenyl ($Bi(Ph)_3$) was used as a metal-organic (MO) CVD precursor.

As detailed in the experimental section, three experiments were performed with identical conditions except run duration (for runs 1 and 2, it was of 2 h; for run 3 it was of 4 h). No change appeared in the size distributions of particles measured by laser granulometry before and after deposition, which means that no particles agglomeration occurred during CVD (see Supplementary Material). According to pressure drop measurements, the fluidization quality was excellent during all runs; this favors the uniformity of treatment on the whole particles of the bed. We verified that elutriation, i.e., loss of particles in the outlet gases, was negligible; therefore the increase in mass of powders was equal to the mass of deposited bismuth oxide. These masses were of 4.5 g for both runs 1 and 2, which indicate that the reproducibility was good, and of 8.8 g for run 3. By assuming uniform deposition around particles, we deduced deposition thicknesses of 135 nm for runs 1 and 2 and of 263 nm for run 3 (calculations are detailed in the Supplementary Material). The sublimator was also weighed after experiments. The masses of $Bi(Ph)_3$ evaporated was found to be around 7.3 g for runs 1 and 2, and 14.6 g for run 3 (these masses are in good agreement with those predicted using the saturation vapor pressure given by Yusha et al.[11]). As a consequence, we obtained $Bi(Ph)_3$ conversions into the fluidized bed of roughly 60%.

As quantitative results provided by energy dispersive X-ray (EDX) analyses on powders have a bad precision,

only a relative comparison of the magnitude of the EDX atomic percentages can be performed to verify the uniformity of deposition (i.e., the presence of bismuth in the various analyzed zones). Figure 1 shows some EDX results after run 3; similar results after run 2 are given in the Supplementary Material. These results are representative of a series of six to eight analyses performed per run, both in various zones of a same grain and for various particles of a same run. Even if not statistically rigorous, they show that bismuth is deposited uniformly over particles.

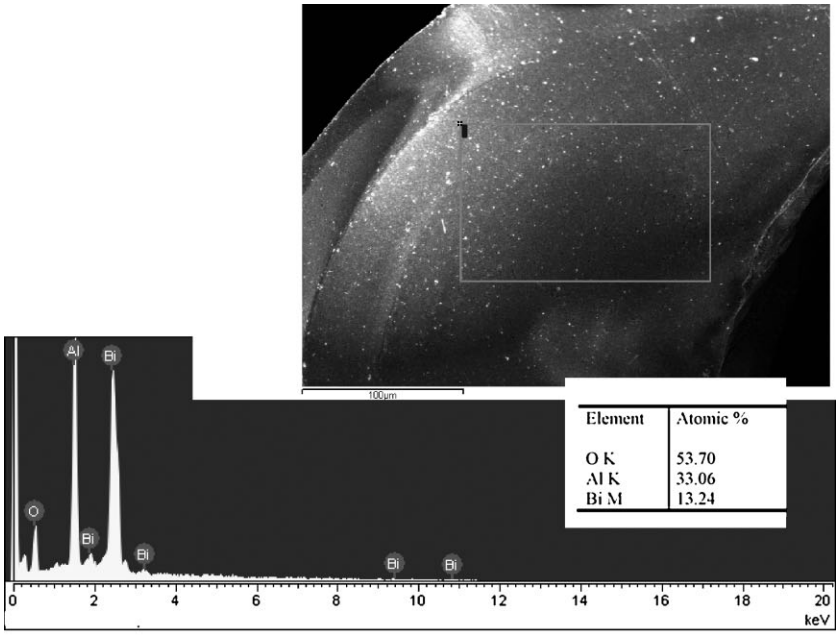

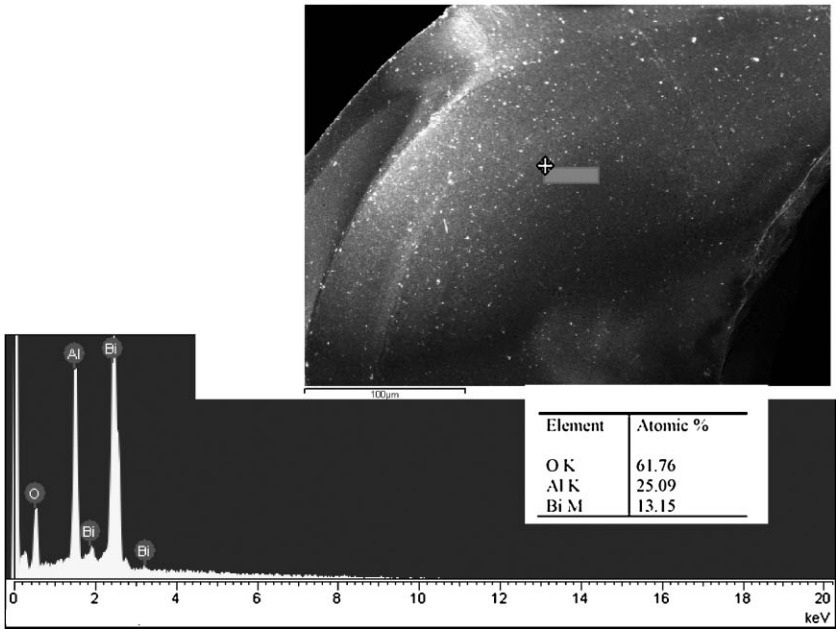

Fig. 1. SEM-EDX results after run 3. a) Average atomic percentages on the square zone of 80 μm × 150 μm, and b) local atomic percentages on the cross of 1 μm × 1 μm.

Details of the XRD pattern of the powder after run 3 are displayed in Figure 2, with the d_{hkl} and the relative intensities of the reference compounds extracted from the ICDD data base. The most intense diffraction peaks are those of the α-Al_2O_3 substrate. Some additional diffraction peaks are also observed, which may be safely indexed as those of α-Bi_2O_3 (reference ICDD 41-1449). The diffraction peaks of the deposited bismuth oxide are relatively broad, and the three peaks around $2\theta = 28^\circ$ (hkl = 111,120, and 021) and the two peaks around $2\theta = 33^\circ$ (hkl = −321 and 231) are not resolved. The bandwidth measured on the main Al_2O_3 peak is considered here as the instrumental bandwidth. The additional broadening on Bi_2O_3 (0.30 to 0.15° on 2θ scale) has been employed to estimate, with the Scherrer formula, an average crystallite size of 40 ± 10 nm. This value is close to those obtained by Bedoya et al.[1] The presence of another phase is suspected; the narrow peak at $2\theta = 24.64^\circ$ and the broader one at 30.46° are well consistent with the cubic (γ) phase. The positions and intensities of β-Bi_2O_3 (reference ICDD 27-050) are also schematized in Figure 2 since it has been reported in several previous works.[1,2] However, from the XRD investigation, there is no clear evidence of this phase in our samples.

An investigation by Raman spectroscopy was also performed. In Figure 3, a typical spectrum of the powder after run 3 is displayed. It is compared with the one observed on the pure alumina powder before deposition and with that of α-Bi_2O_3 powder, as a reference. The spectrum observed on the alumina substrate displays some narrow and relatively weak features that have been very well documented; they are assigned to vibration modes of the corundum structure[13] at 378, 418, 432, 451, 578, 645, and 751 cm^{-1}. Broad and more intense features are also observed on the high wave number side of the spectrum; they are due to the luminescence of some Cr^{3+} impurities naturally present in alumina. These features at 650 and 860 cm^{-1} in Raman shift units are shoulders of the very intense, so-called Ruby R-doublet at 694.3-692.8 nm. Under our experimental conditions (excitation at 633 nm), the R-doublet is observed at 1365–1395 cm^{-1} in Raman shift units; it is not shown here because it is outside the region of interest.

After run 3, all the features due to the substrate are still observed, together with a

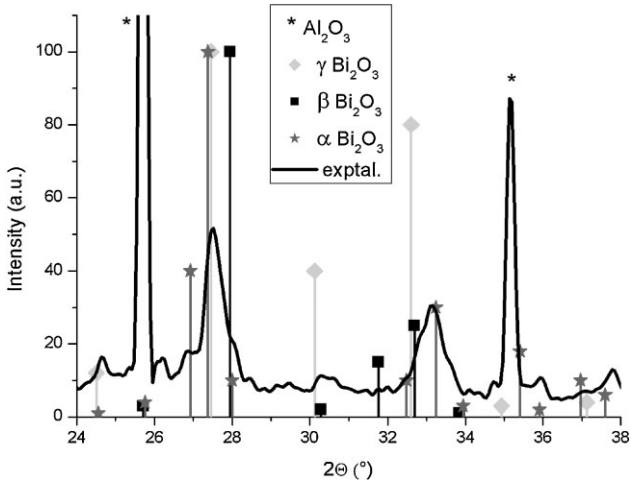

Fig. 2. Details of the XRD plots of the powder after run 3. Symbols from ICDD cards 45-1344 (γ-Bi_2O_3), 27-050 (β-Bi_2O_3), 41-1449 (α-Bi_2O_3), and 10-0173 (α-Al_2O_3).

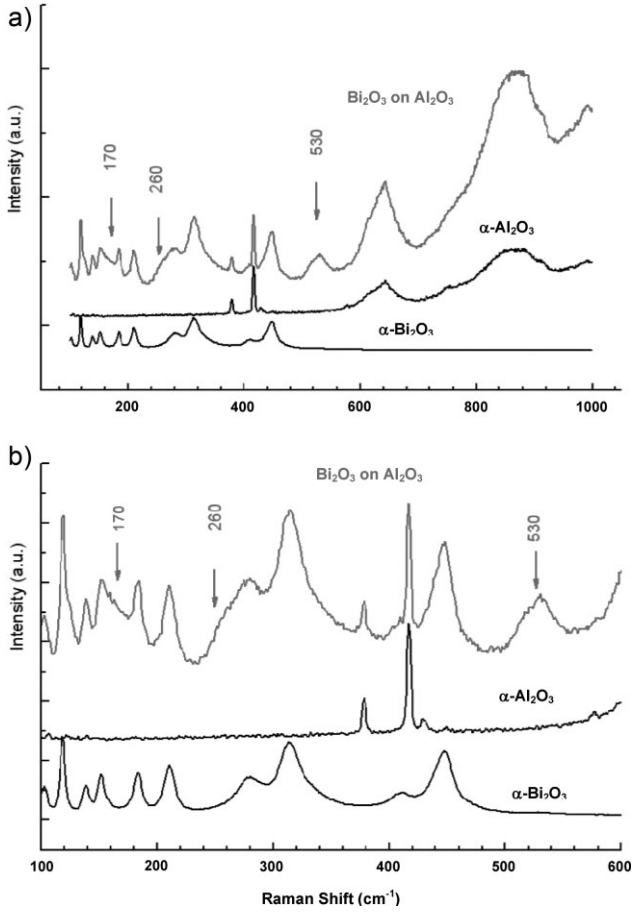

Fig. 3. Room temperature Raman spectra of the powder obtained after run 3 under excitation by He-Ne radiation at 633 nm. The spectra recorded on the alumina powder before deposit and on a reference α-Bi_2O_3 are also displayed. a) Spectra recorded up to a 1000 cm^{-1} Raman shift, showing the luminescence from Cr^{3+} impurities in alumina (see text). b) Details of the range 100–600 cm^{-1}. The numerical values and arrows indicate features from γ-Bi_2O_3.

set of well-defined peaks which match very well those of the α-Bi_2O_3 powder. The assignment of all Raman active modes has been performed by Narang et al. [14] The peak wave numbers observed here for the reference as for the run 3 powder, agree nicely with previously reported values at 103, 119, 138, 151, 184, 210, 279, 314, 408, and 447 cm^{-1}. Besides these components, additional features are also observed for the deposited films; there is a broad and well-isolated peak at 530 cm^{-1}, and shoulders around 260 and 170 cm^{-1}. Hardcastle and Wachs[15] have reported the Raman spectra of β and δ, and have analyzed them in terms of molecular structure of Bi-O_n polyhedra. One of their conclusions is that the Bi-O_n polyhedron in β is similar to that found in α (i.e. the β peaks cannot easily be distinguished from the α peaks), while those in δ are more closely related to the sillenite-type γ-Bi_2O_3. The sillenite phases, i.e., $Bi_{12}SiO_{20}$[16], exhibit Raman stretches at 527–538, 310–373, and 127–139 cm^{-1}, well in the ranges where we have observed additional modes in our samples; the investigation by Raman spectroscopy then confirms that the deposits are a mixture of α- and γ -Bi_2O_3. There is no feature proving the presence of β.

Finally, the powders after runs 2 and 3 were observed by scanning electron microscopy (SEM). Figure 4a shows the surface of an alumina particle of the initial powder; we can distinguish rather smooth zones on the left and striated zones on the right. Note that after deposition with low magnification, it was still possible to make the distinction between initially smooth or striated zones despite the presence of the film. On Figures 4b and 4c, we can observe the film of Bi_2O_3 deposited on the same alumina particle (after run 2) but in different zones. In Figure 4b, the deposition occurred on a smooth zone and the film of Bi_2O_3 is rather uniform, whereas on Figure 4c, the deposition occurred on a striated zone, and the morphology of the film is more structured and shows some heterogeneities. This trend was also observed for run 3 (more SEM images before and after CVD for runs 2 and 3 are presented as Supplementary Material). We can then deduce that the topography of the films of Bi_2O_3 deposited was dependent of the state of the initial surface. This is a rather surprising result for so thick films (about 100 nm). This probably means that these films are highly conformal. According to Bandoli et al., [2] there is not a marked difference between Bi_2O_3 and Al_2O_3 nucleation sites due to chemical similarity between the two oxides. This could explain the phenomena observed. The only operating parameter which has been varied in this study is the deposition time. It appears that it has no influence on the morphology of the deposition (see Supplementary Material).

In conclusion, Bi_2O_3 films have been deposited on the surface of alumina particles by FBCVD under atmospheric pressure, using bismuth triphenyl and oxygen as precursors. For the operating range tested, the presence of Bi on the whole particles has been evidenced by EDX, and the existence of the α and γ phases of Bi_2O_3 has been revealed

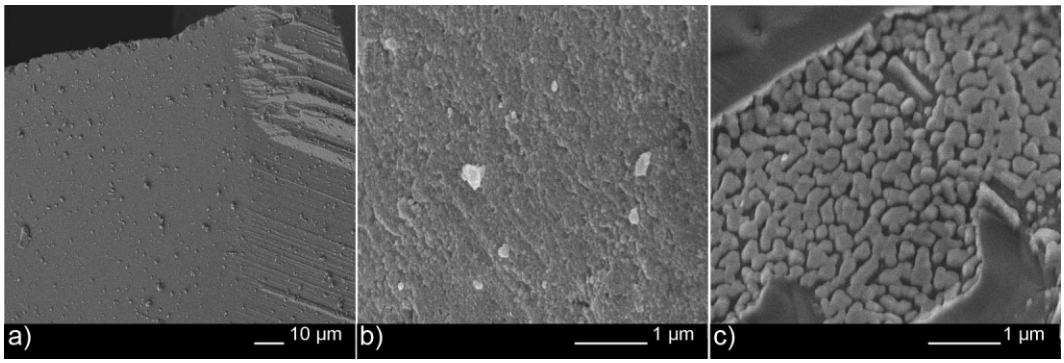

Fig. 4. SEM images of the surface of a) a pure alumina particle, b) and c) a particle obtained after run 2 viewed in two different zones.

consistently by Raman spectroscopy and by XRD. This study seems to be the first one reporting the synthesis of Bi_2O_3 from $Bi(Ph)_3$ by MOCVD under atmospheric pressure and on powders. New work is in progress to perform this deposition on ZnO submicrometer scale particles by vibrated FB-CVD in order to develop new generations of varistors.[17]

Experimental

The experimental equipment is presented in detail elsewhere [18]. It consisted of a vertical cylindrical steel column; its internal diameter and height were 0.05 m and 0.7 m, respectively. At the bottom of the column, a porous steel plate provided a homogeneous gas distribution. The reactor was externally heated by a two-zone electrical furnace. Fluidized bed temperatures were monitored using central thermocouples which indicated the axial profile of temperature in the reactor. A differential pressure gauge measured the pressure drop existing between the bottom part of the reactor (under the distributor) and its top part. Experiments have been performed under atmospheric pressure. The differential pressure drop and bed temperatures were monitored continuously using a computerized data acquisition system.

A sublimator containing the $Bi(Ph)_3$ precursor was immersed in a thermostated oil bath. By a first gas line (line A), a nitrogen flow passed through the sublimator and was then sent to the bottom of the column, below the distributor. A second gas line (line B) canalized a flow of nitrogen and oxygen directly to the bottom of the column. Gas flow rates were controlled by rotameters. Heating ribbons were rolled up around the gas lines to preheat gas and to avoid re-condensation of $Bi(Ph)_3$ vapor. Temperatures of the thermostatted bath and of the heating ribbons were fixed to 150 °C. In lines A and B, nitrogen flow rates were equal to 6 slm and 7.15 slm respectively. The oxygen flow rate in line B was equal to 10 vol. % of the total gas flow rate. For each experiment, initially, 21 g of $Bi(Ph)_3$ were put in the sublimator and 800 g of non-porous alumina powder in the fluidization column (leading to a fixed bed height on column diameter ratio equal to 4). The total gas flow rate (13.15 slm) just corresponded about three times the minimum fluidization velocity of the powder at the operating temperature.

During the FB-MOCVD process, clogging of the inlet gas lines and of the distributor either by the precursor condensation or by its decomposition is a frequent issue. After a fine tuning of the whole process temperatures, including those of the inlet gas lines, this did not happen during our experiments.

The powders before and after CVD were analyzed as follows:

- Laser scattering size analyses of particles after air-dispersion under an over pressure of 4 bars were performed with a MasterSizer2000 Malvern setup. Each measurement corresponds to an average value calculated over 3 runs.
- The powder morphology was observed (i) by SEM on a LEO 435 VP on which EDX measurements were also performed, and (ii) by field effect gun (FEG) SEM using a JEOL 6700S.
- The crystalline state of the materials was analyzed by X-ray diffraction (XRD) using a diffractometer (SEIFERT 3000TT).
- The nature of the depositions was studied by Raman spectroscopy using a Labram HR800 (Jobin Yvon), in the micro-Raman configuration, with an He/Ne laser as light source.

[1] C. Bedoya, G. G. Condorelli, G. Anastasi, A. Baeri, F. Scerra, I. L. Fragalà, *Chem. Mater.* **2004**, *16*, 3176.

[2] G. Bandoli, D. Barreca, E. Brescacin, G. A. Rizzi, E. Tondello, *Chem. Vap. Deposition* **1996**, *2*, 238.

[3] A. Cabot, A. Marsal, J. Arbiol, J. R. Morante, *Sens. Actuators B* **2004**, *99*, 74.

[4] M. Schuisky, A. Härsta, *Chem. Vap. Deposition* **1996**, *2*, 235.

[5] A. Pan, A. Ghosh, *J. Non-Cryst. Solids* **2000**, *271*, 2157.

[6] S. W. Kang, S. W. Rhee, *Thin Solid Films* **2004**, *468*, 79.

[7] M. Schuisky, A. Hårsta, *J. Electrochem. Soc.* **1998**, *145*, 4234.

[8] T. Takeyama, N. Takahashi, T. Nakamura, S. Itoh, *Surf. Coat. Technol.* **2006**, *200*, 4797.

[9] M. Mehring, *Coord. Chem. Rev.* **2007**, *251*, 974.

[10] D. Barreca, G. A. Rizzi, E. Tondello, *Thin Solid Films* **1998**, *333*, 35.

[11] S. Yusha, K. Kikuchi, M. Yoshida, K. Sugawara, S. Shiohara, *Mol. Cryst. Liq. Cryst.* **1990**, *184*, 231.

[12] A. Harvig, A. G. Gerards, *Thermochim. Acta* **1979**, *28*, 121.

[13] S. P. S. Porto, R. S. Krishnan, *J. Chem. Phys.* **1967**, *47*, 1009.

[14] S. N. Narang, N. D. Patel, V. B. Kartha, *J. Mol. Struct.* **1994**, *327*, 221.

[15] F. D. Hardcastle, I. E. Wachs, *J. Solid State Chem.* **1992**, *97*, 319.

[16] R. J. Betsch, W. B. White, *Spectrochim. Acta* **1978**, *A34*, 505.

[17] W. Onreabroy, N. Sirikulrat, *Mater. Sci. Eng. B* **2006**, *130*, 108.

[18] L. Cadoret, N. Reuge, S. Pannala, M. Syamlal, C. Coufort, B. Caussat, *Powder Technol.* **2009**, *190*, 185.